PHILOSOPHICAL TRANSACTIONS OF THE ROYAL SOCIETY A MATHEMATICAL, PHYSICAL & ENGINEERING SCIENCES

Past, present and impendent hydroelastic challenges in the polar and subpolar seas

Vernon A. Squire

Phil. Trans. R. Soc. A 2011 **369**, 2813-2831
doi: 10.1098/rsta.2011.0093

PHILOSOPHICAL TRANSACTIONS OF THE ROYAL SOCIETY A

Phil. Trans. R. Soc. A (2011) **369**, 2813–2831
doi:10.1098/rsta.2011.0093

Past, present and impendent hydroelastic challenges in the polar and subpolar seas

By Vernon A. Squire*

Academic Division, University of Otago, PO Box 56, Dunedin 9054, New Zealand

Current and emergent advances are examined on the topic of hydroelasticity theory applied to natural sea ice responding to the action of ocean surface waves and swell, with attention focused on methods that portray sea ice more faithfully as opposed to those that oversimplify interactions with a poor imitation of reality. A succession of authors have confronted and solved by various means the demanding applied mathematics associated with ocean waves (i) entering a vast sea-ice plate, (ii) travelling between plates of different thickness, (iii) impinging on a pressure ridge, (iv) affecting a single ice floe with arbitrarily specified physical and material properties, and (v) many such features or mixtures thereof. The next step is to embed simplified versions of these developments in an oceanic general circulation model for forecasting purposes. While targeted on specific sea-ice situations, many of the reported results are equally applicable to the interaction of waves with very large floating structures, such as pontoons, floating airports and mobile offshore bases.

Keywords: hydroelasticity; sea ice; ocean surface waves; general circulation model

1. Introduction

The polar oceans have changed over the last 20 years and they continue to evolve. In the past, central Arctic Basin sea ice was, by and large, continuous but intersected by a network of meandering imperfections such as open or refrozen leads and pressure ridges, and the occasional polynya. Ice concentration was normally high and the average floe size was very large in medial regions, but near the margins or in regions of deformation or shear, smaller floes could be distinguished and the sea ice would typically be less compact. While warmer summer temperatures undoubtedly caused melting, a significant proportion of Arctic Basin sea-ice survived the æstival onslaught to become heavily deformed multi-year ice that circumgyred the polar mediterranean basin before exiting at Fram Strait or the northern Barents Sea. Near ice-free areas, in regions where open ocean processes are influential such as the northern Greenland Sea, surface waves and swells penetrated the pack ice with sufficient intensity to fracture local ice floes and regulate their size but, apart from the longest swells, they were soon attenuated before reaching the deep ice interior [1,2].

*vernon.squire@otago.ac.nz.

One contribution of 13 to a Theme Issue ‘The mathematical challenges and modelling of hydroelasticity’.

In the winter Southern Ocean, recalling that the vast proportion of sea ice here is first year ice that disintegrates during the austral summer, the ice cover appearance is typically quite different. In the Weddell Sea, for example, pancake ice plays a substantial role, contained again in size by aggressive incoming ocean waves that originate far to the north. Beyond this often expansive band of pancakes, after the ferocity of the incoming waves has calmed sufficiently to allow adjacent floes to bond together using nearby frazil ice as 'glue', much larger floes characteristic of interior sea ice are seen. While their congelation growth thickness is modest—perhaps only 0.5 m or so, these floes are often very rough, with jagged uneven bottoms due to rafted pancakes doubling or tripling the normal ice thickness, and with the edges of pancakes protruding upwards to give a surface topography resembling a 'stony field' [3].

The onset of global climate warming has strongly influenced sea-ice morphology. This is particularly evident in the Arctic Ocean during summer, where concentration and thickness have both diminished anomalously during the last 20 years [4,5], with the ice becoming more fragmented like a marginal ice zone (MIZ; see §5). This has undoubtedly occurred because of warmer temperatures that cause melting on the upper surfaces of ice floes, which encourages further melting because of the enhanced absorption owing to the lowered average albedo of melt water pools and water-infiltrated snow. But an attendant contribution comes from an increased capacity for ocean waves and swell to damage the ice. This arises primarily because the character of the sea-ice cover has altered from being 'quasi-continuous' to being MIZ-like and the ice itself has become weakened by the thermal assault. Accordingly, the destructive payload of the waves penetrates further—leading to altered fluxes between the atmosphere and ocean, but it will also be associated with the heightened and more frequent extreme events we are experiencing owing to climate change, which will potentially lead to higher waves being created at distant storm centres. In addition, direct wave-induced melting of ice floes will occur more readily in the manner described by Wadhams *et al.* [6]. The strong positive feedback due to albedo reduction and ocean-wave breakup suggests that the summer Arctic is unlikely to revert to its former configuration easily. Interestingly, in winter, the waves and swell that assist in regulating ice floe size will actually enhance further congelation ice growth by creating more open leads that quickly freeze over with new ice.

We know a great deal less about how Antarctic sea ice is adapting, and it may even have increased in overall extent over the last two decades. Unlike the Arctic, which is an ocean basin surrounded by land with sea ice extending all the way to the Pole, the Antarctic is a large continent surrounded by ocean where the sea ice has more room to expand in the winter. Since the start of the satellite record, total Antarctic sea ice appears to have increased by about 1 per cent per decade, but whether this small overall increase in extent is a sign of meaningful change in the Antarctic is uncertain because ice extents in the Southern Hemisphere vary considerably from year to year and from place to place around the continent. Considered individually, only the Ross Sea sector had a significant positive trend, while sea-ice extent has actually decreased in the Bellingshausen and Amundsen Seas [7]. Further uncertainty arises because these conclusions relate to extent and concentration only, as the time series on which they are based is constructed using radiometers that measure microwave energy

radiated from the Earth's surface. Changes in sea-ice morphology are not easily detected unless accompanied by a change in the compactness of the ice cover. Consequently, we are unable to confirm or reject the notion that sea-ice physical properties other than concentration and extent, e.g. ice thickness, ductility, floe size distribution or the width of the pancake ice band, have altered akin to changes in the Arctic. However, the natural variability of Antarctic sea ice, together with the continuous pounding it receives from a wave climate that is methodically intensifying because of global warming, does suggest that ice properties around the continent will have evolved.

We are making the case in this paper that the recurring interactions that occur between ocean waves and swell and sea ice are a universal element of the polar and subpolar seas that is crucial to understanding how ice covers mutate, and that this is especially relevant in the context of a warmer Earth where sea ice will be emasculated and ocean waves are more violent. Yet remarkably, there is currently no observation system for ocean waves in ice-covered seas, state-of-the-art operational models such as the European Centre for Medium-range Weather Forecasts Wave Prediction Model do not simulate wave propagation into ice-covered areas, and operational sea-ice models do not accommodate wave effects either, despite their acknowledged influence on MIZ dynamics. We expect future offshore operations in Arctic waters to take place more frequently in areas of seasonal ice cover, which will necessitate integrated weather, waves, ocean and sea-ice monitoring and forecasting systems for safer functionality. The hazards involved in offshore polar exploration, like collisions with icebergs and dangerous sea-ice conditions, are considerably amplified when aggressive ocean waves coerce the ice into motion and emergency situations may arise where operations on vessels or platforms and production must be interrupted and environmental degradation occurs. And, although not imminent, it is probable that these sentiments will apply to Southern Ocean ice fields in the future as well.

An expedient paradigm shift has occurred over the last several years in relation to modelling how surface ocean waves and swells communicate with sea ice, either agglomerations of floes in an MIZ or continuous ice sheets fenestrated by leads and intersected by pressure ridges. For the first time, prescribed model terrain closely resembles natural sea ice with its considerable heterogeneity and irregularity. In the Arctic Basin, for example, wave trains have been tracked for nearly 2000 km [2,8], while in the MIZ, fully three-dimensional models are now beginning to accurately compute the embrangled exchanges that occur between compliant ice floes in motion. Moreover, the first serious attempts to embed ocean-wave–sea-ice interactivity into an oceanic general circulation model (OGCM) are occurring, as it is now recognized that the accurate parametrization of how waves affect pack ice, and vice versa, can significantly influence the accuracy of model outcomes.

Hereinafter, we will introduce and briefly explain the theoretical analyses that have progressed our current understanding of wave propagation in fields of sea ice. Because sea-ice plates are compliant and are known to flex (and routinely fracture) under wave action, collectively the work described embodies the modern topic of hydroelasticity—defined as the branch of science that is concerned with the motion of deformable bodies in liquids. Beginning in §2 with a helpful canonical model, we will then, in turn, discuss continuous sea ice (§3), discrete finite ice floes of different sizes and shapes (§4), aggregations of floes

forming MIZs (§5), the datasets that can be used for model validation (§6) and, finally, how hydroelastic representations of scattering can be assimilated into OGCMs (§7).

2. Canonical model

First consider (figure 1) what happens when waves propagating on the free ocean surface enter or leave a sea-ice-covered region that may be either semi-infinite $x \in [0, \infty)$ or of finite breadth $x \in [0, d]$, where $y \in (-\infty, \infty)$. This canonical problem can be modified later to allow for a continuous sea-ice plate. The uniform Euler–Bernoulli elastic thin plate [9] is used most frequently to describe how the ice sheet bends under the wave action, with viscosity included when hysteresis is perceptible during flexure [10]. Plate thickness is denoted by h; mass per unit area by $m = \rho' h$, where ρ' is the density; and rigidity by $D = Eh^3/12(1-\nu^2)$, where E is Young's modulus and ν is Poisson's ratio. The lower surface of the plate is described by $z = \zeta(x, y, t)$, where t is time. Assuming that the water is inviscid and incompressible and that the flow is irrotational and undergoes small amplitude motions, a velocity potential $\Phi(x, y, z, t)$ can be defined such that $\nabla^2 \Phi = 0$, $\nabla = (\partial_x, \partial_y, \partial_z)$ in the fluid and $\Phi_z = 0$ on the sea floor $z = -H$. The pressure $p(x, y, z)$ is accessible from the linearized Bernoulli equation, i.e.

$$p = p_{\mathrm{a}} + mg - \rho \Phi_t - \rho g z, \tag{2.1}$$

where g is the acceleration owing to gravity and p_{a} is the constant atmospheric pressure. If ∇_{h}^4 denotes the biharmonic operator in the xy-plane,

$$p|_{z=\zeta} = p_{\mathrm{a}} + mg + D\nabla_h^4 \zeta + m\zeta_{tt}, \tag{2.2}$$

where an Euler–Bernoulli plate is assumed and $\nabla_h = (\partial_x, \partial_y)$. Equations (2.1) and (2.2) are combined on $z = \zeta$ and linearized about $z = 0$ to give

$$D\nabla_h^4 \zeta + \rho g \zeta + m\zeta_{tt} + \rho \Phi_t = 0 \quad \text{on } z = 0, \tag{2.3}$$

with additional coupling between fluid and floe described by the kinematic condition $\zeta_t = \Phi_z$, also linearized about $z = 0$. Denoting the angular frequency by ω and incorporating the shift invariance in the y-direction, we assume that $\Phi(x, y, z, t) = \mathrm{Re}[-\mathrm{i}\omega\phi(x, z)\mathrm{e}^{\mathrm{i}(ly-\omega t)}]$ and $\zeta(x, y, t) = \mathrm{Re}[w(x)\mathrm{e}^{\mathrm{i}(ly-\omega t)}]$. Then, the wavenumber l is related to θ and

$$(D(\partial_x^2 - l^2)^2 + \rho g - m\omega^2)w - \rho\omega^2\phi = 0, \quad w = \phi_z|_{z=0}. \tag{2.4}$$

Most authors prefer to work with non-dimensionalized quantities. Here, we non-dimensionalize length with respect to the natural length $L = \sqrt[5]{D/\rho\omega^2}$ and time with $\tau = \sqrt[8]{D/\rho g^5}$, which has the advantage of simultaneously assimilating the properties of both the ice floe and the wave and of furnishing a dispersion relation in terms of a single parameter (see [11]). Defining $\lambda = g/L\omega^2$, $\mu = m/\rho L$, writing $(\bar{\boldsymbol{x}}, \bar{t}) = (\boldsymbol{x}/L, t/\tau), \bar{\phi}(\bar{x}, \bar{z}) = \phi(x, z)/L^2, \bar{w} = w/L, \bar{H} = H/L, \bar{l} = l/L$, and henceforth dropping the overbars to avoid clutter, our now non-dimensionalized

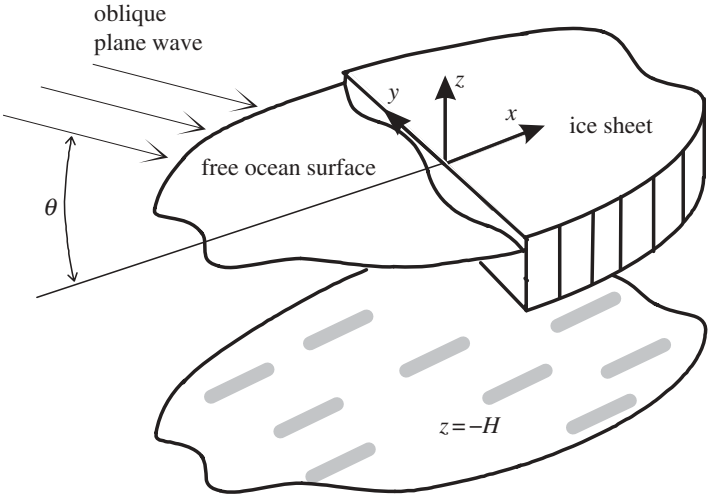

Figure 1. Open water waves impinge obliquely onto a compliant ice sheet that is either semi-infinite or of finite length d in the x-direction, but extends to $\pm\infty$ in the y-direction. The coordinate frame is shown schematically, as in most cases, ice draft will be assumed to be negligible with $z=0$ located at the mean free surface and $z=-H$ at the sea floor.

$\phi(x,z)$ must satisfy

$$(\nabla^2 - l^2)\phi(x,z) = 0, \tag{2.5a}$$

$$\mathcal{L}(x,\partial_x)w(x) - \phi(x,0) = 0, \tag{2.5b}$$

$$w(x) - \phi_z(x,0) = 0 \tag{2.5c}$$

and

$$\phi_z(x,-H) = 0. \tag{2.5d}$$

Operator $\mathcal{L}(x,\partial_x) = (\partial_x^2 - l^2)^2 + \lambda - \mu$ beneath the ice and is equal to λ in open water, so equation (2.5*b*) actually expresses two equations if we define

$$\mathcal{L}(x,\partial_x) = \alpha(\partial_x^2 - l^2)^2 + \lambda - \mu\beta, (\alpha,\beta) = \begin{cases} (0,0) & \text{in open water,} \\ (1,1) & \text{beneath the ice.} \end{cases} \tag{2.6}$$

Because energy is conserved at any interior free edge, $x = x_0$, we must also have

$$\mathcal{L}_-(\partial_x)w(x_0) = \mathcal{L}_+(\partial_x)w_x(x_0) = 0, \quad z = 0, \tag{2.7}$$

where $\mathcal{L}_\pm(\partial_x) = (\partial_x^2 - l^2) \mp (1-\nu)l^2$. And, referring to figure 1, radiation conditions as $x \to \pm\infty$ are necessary to close the system, namely

$$\phi(x,z) \sim \begin{cases} (\mathrm{e}^{\mathrm{i}kx} + R\mathrm{e}^{-\mathrm{i}kx})\varphi(z) & \text{as } x \to -\infty, \\ T\mathrm{e}^{\mathrm{i}\kappa x}\,\varphi(z) & \text{as } x \to \infty, \text{ for a semi-infinite sheet, or,} \\ T\mathrm{e}^{\mathrm{i}kx}\varphi(z) & \text{as } x \to \infty, \text{ for a finite solitary floe,} \end{cases} \tag{2.8}$$

where the quantities R and T are called the reflection and transmission coefficients. The wavenumbers corresponding to the (lossless) propagating mode for open water and the ice plate are, respectively, $K=(k^2+l^2)^{1/2}$ and $\gamma=(\kappa^2+l^2)^{1/2}$, where k and κ are their respective components in the x-direction and the relationship $l=k\tan\theta=K\sin\theta$ holds.

Finally, a useful power flow condition can be expressed using far-field energy flux arguments,

$$s|T|^2=1-|R|^2, \quad \text{such that} \begin{cases} s\neq 1 & \text{for a semi-infinite sheet,} \\ s=1 & \text{for a finite solitary floe,} \end{cases} \tag{2.9}$$

where s is known as the intrinsic admittance.

3. Continuous ice

In regions that are protected from the full impact of the open ocean, by land, a barrier of unconfined pack ice or simply because of distance, sea ice will invariably consolidate into a zone composed of vast ice floes that is virtually continuous. This is not to say that the sea ice is homogeneous or isotropic; indeed, it is not. But rather that to penetrating ocean waves, the length scales associated with the ice cover are large enough and its integrity is sufficiently high that the medium may be regarded as quasi-continuous with random imperfections. These flaws may be meandrous cracks, open or refrozen leads, the occasional polynya, or sinuous pressure ridge sails and keels. These are quite distinct circumstances to wave propagation through a band of loose ice floes, where waves are scattered by the edges of discrete 'rafts' that are also free to respond as autonomous compliant floating bodies and wavelengths are of the same order as floe diameters.

The synthesis of Squire [12], a cognate study focused on offshore engineering hydroelasticity [13], and an earlier review [1] have extended sections on wave propagation through continuous sea ice, although the bulk of the reported work is theoretical as few experiments have been done. We do not intend to rehash these works, although there is inevitably some overlap and the same single theoretical framework advanced in the earlier papers will be used.

(a) Cracks

Suppose that the ice sheet now covers the entire ocean surface, but that it has N parallel cracks located at points $x=x_n$ within a closed finite interval $[0,d]$. Then, only minor changes need to be made to the equations of §2, as follows:

— equations (2.5) remain the same;
— $\mathcal{L}(x,\partial_x)=(\partial_x^2-l^2)^2+\lambda-\mu, \quad x\in(-\infty,\infty)\setminus\bigcup\{(x_n^-,x_n^+)\}$ in equation (2.6);
— $\mathcal{L}_-(\partial_x)w(x_n^\pm)=\mathcal{L}_+(\partial_x)w_x(x_n^\pm)=0$ for each x_n in equation (2.7);
— equation (2.8) becomes $\phi(x,z)\sim\begin{cases}(\mathrm{e}^{\mathrm{i}\kappa x}+R\mathrm{e}^{-\mathrm{i}\kappa x})\varphi(z) & \text{as } x\to-\infty,\\ T\mathrm{e}^{\mathrm{i}\kappa x}\varphi(z) & \text{as } x\to\infty;\end{cases}$ and
— $s=1$ in equation (2.9) because the ice cover extends from $-\infty$ to ∞.

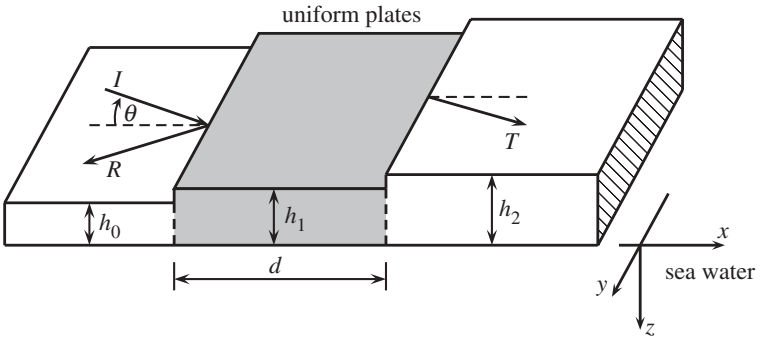

Figure 2. Two semi-infinite elastic ice plates of thickness h_0 and h_2 surround a finite elastic plate of thickness h_1. The thickness of any of the three plates may be set to zero. Axes are displaced to the right to avoid clutter. Williams & Squire [14]. Reproduced by permission of Cambridge University Press.

(*b*) *Open lead*

A lead forms when a crack opens owing to divergent forces brought about by winds and currents acting upon the ice plate over large spatial scales. Leads are common features of polar ice fields and, when temperatures are low, they quickly freeze over to create an ice sheet intermediate between the two existing plates. Incident waves are partially reflected to a degree that depends on the configuration and properties of the lead. In its simplest form, i.e. for an open lead of width $2d$, the boundary-value problem to be solved is again an amended version of §2, as follows:

— equations (2.5) remain the same;
— equation (2.6) is the same but with $(\alpha,\beta)=\begin{cases}(0,0) & \text{for } |x|<d,\\ (1,1) & \text{for } |x|>d;\end{cases}$
— equation (2.7) becomes $\mathcal{L}_-(\partial_x)w(\pm d)=\mathcal{L}_+(\partial_x)w_x(\pm d)=0$;
— equation (2.8) is the same as for a crack; and
— $s=1$ in equation (2.9) again.

(*c*) *Steps in thickness*

The situation shown in figure 2 is described by the following modifications to our canonical boundary-value problem in §2:

— equations (2.5) and (2.9) remain the same;
— equation (2.6) remains the same but with $(\alpha,\beta)=\begin{cases}(\alpha_0,\beta_0) & \text{for } x<0,\\ (\alpha_1,\beta_1) & \text{for } 0<x<d,\\ (\alpha_2,\beta_2) & \text{for } x>d,\end{cases}$
such that L and μ are now each defined for the plate with the largest flexural rigidity and α and β are normalized with respect to their respective values for that plate;

— for the edges $x_e = \{0, d\}$, equation (2.7) becomes either $\mathcal{L}_-(\partial_x)w(x_e^\pm) = \mathcal{L}_+(\partial_x)w_x(x_e^\pm) = 0$, for free edges, or, for frozen-together plates,

$$w(x_e^+) = w(x_e^-),$$
$$w_x(x_e^+) = w_x(x_e^-),$$
$$\alpha(x_e^+)\mathcal{L}_-(\partial_x)w(x_e^+) = \alpha(x_e^-)\mathcal{L}_-(\partial_x)w(x_e^-)$$
and $$\alpha(x_e^+)\mathcal{L}_+(\partial_x)w_x(x_e^+) = \alpha(x_e^-)\mathcal{L}_+(\partial_x)w_x(x_e^-);\ \text{and}$$

— equation (2.8) becomes $\phi(x, z) \sim \begin{cases} (e^{ik_0 x} + Re^{-ik_0 x})\varphi_0(z) & \text{as } x \to -\infty, \\ Te^{ik_2 x}\varphi_2(z) & \text{as } x \to \infty. \end{cases}$

(*d*) *Variable terrain*

Williams & Squire [11] incorporated a region of variable properties, expressed through the flexural rigidity and density, in an otherwise uniform ice sheet (figure 3), by redefining the operator (2.6) as

$$\mathcal{L}(x, \partial_x) = (\partial_x^2 - l^2)(\alpha(\partial_x^2 - l^2)) + (1 - \nu)l^2\partial_x^2\alpha + \lambda - \mu\beta, \tag{3.1}$$

where

$$(\alpha, \beta) = \begin{cases} (\alpha(x), \beta(x)) & \text{for } x \in (0, d), \\ (1, 1) & \text{for } x \notin (0, d). \end{cases}$$

The ends of the variable region are welded to the surrounding sheets, so for any point $x = x_c$ where the two regions meet

$$w(x_c^+) = w(x_c^-), \tag{3.2a}$$
$$w_x(x_c^+) = w_x(x_c^-), \tag{3.2b}$$
$$\alpha(x_c^+)\mathcal{L}_-(\partial_x)w(x_c^+) = \alpha(x_c^-)\mathcal{L}_-(\partial_x)w(x_c^-) \tag{3.2c}$$
and
$$(\alpha(x_c^+)\mathcal{L}_+(\partial_x)\partial_x + \partial_x\alpha(x_c^+)\mathcal{L}_-(\partial_x))w(x_c^+)$$
$$= (\alpha(x_c^-)\mathcal{L}_+(\partial_x)\partial_x + \partial_x\alpha(x_c^-)\mathcal{L}_-(\partial_x))w(x_c^-), \tag{3.2d}$$

where $\mathcal{L}_\pm(\partial_x) = (\partial_x^2 - l^2) \mp (1 - \nu)l^2$, as defined after equation (2.7).

(*e*) *Solutions*

(i) *Single features*

The boundary-value problems defined in §3*a–d* have been tackled by a profusion of ingenious mathematical methods, recognizing that the high order of the plate boundary condition makes finding a solution to each problem especially demanding. Methods used include matched asymptotic expansions, eigenfunction matching in several forms, various approaches founded in the theory of Green's functions and variants on boundary-integral methods, the Wiener–Hopf method, residue calculus, Laplace and Fourier transforms, the Carleman integral equation, Rayleigh–Ritz single and multi-mode decomposition after a variationally based reformulation, spectral methods and more.

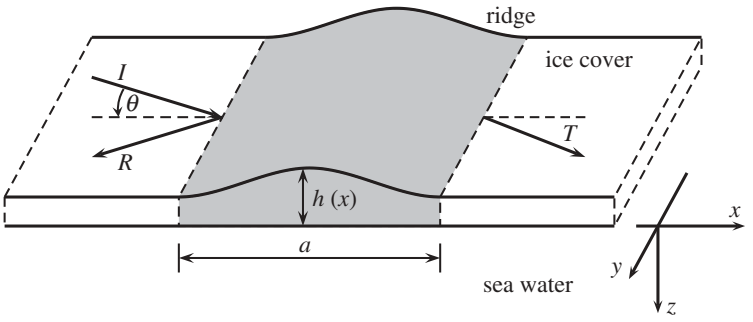

Figure 3. Wave scattering at a pressure ridge. The main ice cover has a constant thickness of h_0 and the sea water has a finite depth of H. The coordinate axes are oriented as shown, but are displaced to the right in the figure so that the y-axis actually corresponds to the left-hand limit of the ridge. Reproduced with permission from Williams & Squire [11].

The astute reader will also have observed that the underside of the ice defined by the Euler–Bernoulli plate boundary condition (2.3) is placed at $z = 0$, which of course is incorrect. In nature, the density of sea ice is such that it has a significant draught, typically about 9/10 of its thickness. While the justification for the zero submergence approximation is defensible, namely that ocean wavelengths are very long compared with the vertical length scale associated with ice thickness so that effects owing to draught will be negligible, the approximation needs to be tested. This was done by Williams & Squire [15] by solving an integral equation arising from a formulation based on Green's functions. Bennetts *et al.* [16] also included Archimedean draught but the focus is mainly on solitary floes. Another paper on the topic is noteworthy. Williams & Porter [17] considered how waves pass through a junction at which two semi-infinite ice sheets of different properties are either frozen together or separated by a crack, allowing the ice sheets to adopt a variable submergence according to thickness. To solve the ensuing integral equation, a series of even Gegenbauer polynomials was employed in a Galerkin scheme, which accommodates the required singularity in the fluid velocity at the junction. This is a clever way of including the correct Archimedean draught with matched eigenfunctions, which facilitates rapid numerical convergence.

(ii) *Multiple features*

Several papers that deal with solitary irregularities, e.g. Williams & Squire [11,14], also go on to consider wave propagation through many such features. To date, however, the most ambitious attempt to achieve this, due to Vaughan *et al.* [8] and Squire *et al.* [2], interfuses the model of Bennetts *et al.* [16] as its kernel. In Squire *et al.* [2], waves were tracked across 1670 km of realistic Arctic sea-ice terrain obtained from upward-looking submarine sonar records (figure 4).

4. Solitary floes

Equations (2.5) with operator (2.6), the finite solitary floe version of equation (2.8) and the free-edge conditions (2.7), are the necessary equations to solve in two dimensions. As for continuous sea ice, this has now been

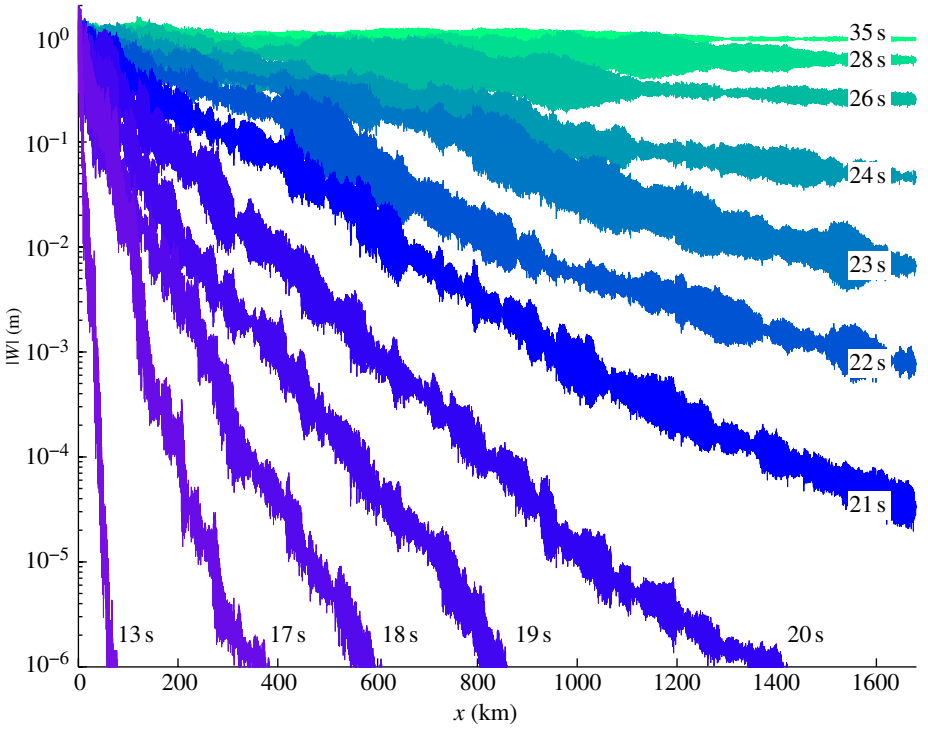

Figure 4. How the amplitude of ocean waves with period ranging from 13 to 35 s is affected by 1670 km of sea-ice terrain. Squire *et al.* [2]. Copyright 2009 American Geophysical Union. Reproduced by permission of American Geophysical Union.

done by a miscellanea of mathematical methods that also nourish the allied, conventionally more temperate, field of very large floating structure research.

However, although the behaviour of two-dimensional isolated floating bodies is interesting, its value is more within the domain of littoral engineering than polar marine physics. A two-dimensional model can be helpful in clarifying aspects of how compliant ice floes bend, or possibly fracture, or parallel structures in an ice field scatter incoming ocean waves, but there is plenty of observational evidence that shows the three-dimensional attributes of scattering in the MIZ are paramount. The MIZ is fundamentally a three-dimensional scattering medium composed of three-dimensional floating bodies, where reflection and transmission causes wave energy to leak laterally rather than directly contributing to the principal wave vector. Accordingly, to capture scattering interactions properly, the elemental floes must, of necessity, be three dimensional. Their motion, deformation and reflective properties provide the scattering kernels of the constituent ice floes that together comprise the MIZ.

A train of long-crested water waves impinging on a single circular raft floating on deep water was studied by Meylan & Squire [18], using two separate eigenfunction methods, and by Andrianov & Hermans [19] for water of any depth. Meylan [20] extended these analyses to allow arbitrary floe shapes using either general vibrational modes specified by means of finite elements or modes specified

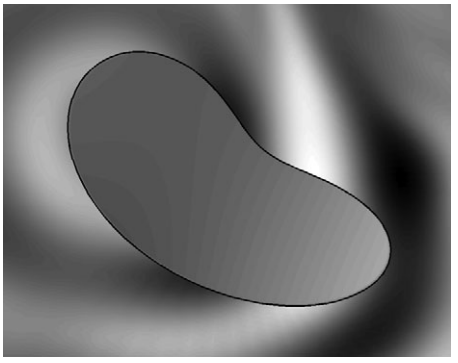

Figure 5. Scattering response of a sea-ice floe. The incident wave propagates from $x \to -\infty$ parallel to the x-axis. The displacement within the floe is shown, along with the surrounding diffracted wave field. Bennetts & Williams [22]. Reproduced by permission of Cambridge University Press.

analytically for restrictive geometries, e.g. a circular thin plate. However, while the compliant circular raft is a good theoretical constituent of an MIZ composed of many floes with randomized floe diameter at specified concentration, to use such a model naively for an MIZ made up of tens of thousands of ice floes would be impractical, even in the unlikely event that the morphology of every floe present was known accurately. Recognizing this challenge, more efficient schemes for computing the wave scattering owing to solitary ice floes have been conceived, e.g. Bennetts *et al.* [21] and Bennetts & Williams [22], and approximate methods for assembling the scattering effects for many floes have been devised.

Bennetts & Williams [22] described a solution method that could be applied to linear wave scattering by a single ice floe or an isolated polynya located in a continuous ice sheet, each requiring a smooth perimeter but for arbitrary shape. Their approach to these problems was based on reducing the spatial dimension in two stages and generated solutions at a low computational cost. Firstly, the governing equations of the full three-dimensional problem were projected onto the horizontal plane using a process of vertical averaging through a Rayleigh–Ritz style approximation. The resulting equations were then converted into sets of one-dimensional integro-differential equations, posed on the boundary between the free surface and the ice-covered fluid, by implementing matrices of Green's functions in conjunction with Green's second identity. This allows the Galerkin technique to be invoked to produce a numerical solution. In figure 5, results obtained using this method show how an ice floe in the shape of a so-called 'crooked egg' scatters a plane incident wave of unit length (in open water) travelling parallel to the x-axis from $x \to -\infty$. The displacements within the scatterer are shown along with the surrounding diffracted wave field, and the effects of the shape of the scattering source on these motions are evident.

5. Fragmented ice

The customary definition of the MIZ is due to Wadhams [23] who described it as the part of the ice cover close enough to the open ocean boundary to be affected by its presence. It is an interfacial region that resides at the fringe of the open and

frozen oceans, neither fully open nor fully frozen over—a mélange of ice cakes and floes, habitually pervaded by slurries of frazil ice and brash. Because the MIZ is a part of the ice cover closest to open sea, it is a very dynamic region that is affected mainly by incoming ocean waves and swells, and changes of wind and current. Concentration is generally variable, both spatially and temporally, and the nature of the ice floes making up the zone is also invariably quite heterogeneous as the waves break up floes differentially or, especially near the ice edge, pummel and raft the ice.

Since energy is dissipated at the ice floes the waves meet during their passage, under steady-state forcing there will be a place in the interior MIZ where the waves lack the ferocity to fracture local floes and, on this account, the ice will remain quasi-continuous. (Indeed the band of wave broken ice created to seaward helps to protect the interior from further wave-induced damage.) That being so, a major way in which the open ocean interacts with sea ice in the region is through wave-induced modification of the underlying floe size distribution, and it is this process that actually produces the MIZ [24]. In a nutshell, the MIZ is formed by ocean waves breaking up the ice floes but, in concert, the belt of ice cakes and modified floes produced shields more remote floes and continuous ice from breaking. Of course, an intensification of wave energy in the open sea beyond the ice edge, caused by the passage of a storm, for example, will lead to further destruction and an altered distribution of floe diameters.

Modelling wave interactions in the MIZ either (i) synthesizes the behaviour of many solitary flexible ice floes or a small number of such floes that are then aggregated to create the complete ice cover or (ii) assumes the zone has certain rheological properties *a priori* and then describes its influence on the waves mathematically. The challenge of (ii) is to find a mathematical representation that encapsulates the physical properties of the MIZ properly, which has never been achieved, although the recent work of Wang & Shen [25] holds promise. Amalgamation of the behaviour of many solitary floes with randomized diameters, three-dimensional shapes and physical properties would therefore appear to be the most prudent approach at this time. As with quasi-continuous sea ice, few field experiments to measure waves in the MIZ have taken place, but it is observed that the attenuation rates of waves travelling in MIZs decrease as the period increases and that a narrow directional spectrum at the ice edge broadens to become isotropic as it evolves with increasing distance into the MIZ (e.g. [24,26,27]).

Although the MIZ is, in detail, a three-dimensional scattering medium, some useful qualitative outcomes can be had from two-dimensional theory. For instance, by means of a wide-spacing approximation, the Williams & Squire [14] theory described in §3*c* can be used to shed light upon how waves travel in a medium composed of many ice plates of different size and thickness separated by open water or thinner ice. This is essentially a two-dimensional MIZ, as an open lead surrounded by ice is the same as two ice floes separating a stretch of open water, once waves local to the edges have dissipated. Exploiting an eigenfunction expansion under each ice floe and matching the expansions at the plate boundaries where free-edge conditions (2.7) must hold, Kohout & Meylan [28] used an equivalent approach. On also comparing with some field data, they concluded that their model, even though two dimensional, is applicable to large floes for short- to medium-wave periods in the 6–15 s range. (See §6 later.)

In a sequence of papers, Peter & Meylan [29–31] and Peter *et al.* [32] applied the seminal exact three-dimensional interaction theory of Kagemoto & Yue [33] to the MIZ, which, in principle, can be real or simulated. The most recent study [31] treated repeated clusters of separate ice floes that lie close together as if they are a single scatterer, emulating the multi-pole method of optics. Periodic structures were also investigated by Bennetts & Squire [34,35], who introduced the added complication of a realistic Archimedean ice floe draught and used periodic Green's functions. The MIZ is, unfortunately, not periodic. While Bennetts *et al.* [36] attempted to overcome this limitation by averaging, the periodicity introduced by artificial recurring structures causes unnatural artefacts such as the creation of extra waves that would not be present in a true MIZ.

Transport theory has also been used to derive an equation for three-dimensional energy transport in the MIZ [37], but for rigid ice floes rather than compliant ones. This method and the independent one of Meylan *et al.* [38] based on a linear Boltzmann equation approach have now been shown to be nearly identical by Meylan & Masson [39] and have produced a linear Boltzmann model for wave scattering in the MIZ.

6. Field and laboratory experiments

The most comprehensive account describing *in situ* observations and experiments relating to wave propagation in fields of sea ice is still due to Wadhams *et al.* [27], noting that this publication includes a reanalysis of the results of Squire & Moore [24] collected in the Bering Sea in 1979. Few experiments have taken place since, although waves have occasionally been measured as a constituent of large-scale experiments focused on understanding several other marine and/or geophysical phenomena (e.g. [40,41]), and there are reports of studies that make use of remote-sensing techniques, such as synthetic aperture radar (SAR) imaging from space (e.g. [42–44]). While, aircraft and satellite-borne remote sensing offers obvious advantages over buoys deployed between or on ice floes, the resolution of current sensors and data analysis and processing complexities have limited their application to date. Indeed, the most convincing study in this regard, namely that due to Wadhams *et al.* [44], concerns wave dispersion in a viscous layer of frazil-pancake ice as opposed to scattering from assemblies of ice floes in an MIZ or a quasi-continuous sea-ice plate, so its relevance to the hydroelastic theme of this volume is less. Notwithstanding this, we remark that the theoretical generalization due to Wang & Shen [25], in which the ice–ocean system was represented by a homogeneous viscoelastic fluid overlying an inviscid layer of finite thickness, where the viscosity is imagined to originate from the frazil ice or ice floes much smaller than the wavelength and the elasticity comes from ice floes that are relatively large when compared with the wavelength, may further improve the interlinking of SAR imagery and theory.

The Wadhams *et al.* [27] datasets were reanalysed by Kohout & Meylan [28] and Bennetts *et al.* [36] to ascertain whether their respective two- and three-dimensional models reproduced similar attenuation rates to those observed by Wadhams *et al.* [27]. Both comparisons with experimental data gave reasonable agreement and provided confidence in each model's ability to describe attenuation due to scattering. However, a recurring deviation is the underprediction of

attenuation for high periods and overprediction at low periods, even though the attenuation coefficients produced by the three-dimensional model do a better job in this respect than those of the two-dimensional model. There are potentially several reasons for this discrepancy, e.g. (i) when the wave amplitude is roughly commensurate with floe size and each is small relative to the wavelength, scattering becomes less important and processes take over that are often described empirically by Morison's equation [45], (ii) even when scattering occurs, there are other processes in the MIZ that cause energy dissipation, e.g. turbulence in the water, breakup and collisions between ice floes, for instance, (iii) sea ice is actually not elastic, it is nonlinearly viscoelastic, and (iv) there is no doubt that a major impediment to making a proper quantitative validation of theory against experiment is the lack of documented detail and level of accuracy about local pack ice morphology at the time when the field experiments took place.

A small number of laboratory experiments have been carried out to observe how waves are affected by 'ice floes', which may be artificial, typically manufactured from a flexible plastic, or real ice if a freezable wave flume is available. The first experiments, done by Wadhams [46] using empty film canisters as floats, demonstrated unequivocally that such experiments were difficult to execute but were nonetheless extremely useful to making sense of how scattering modifies an incoming wave train under controlled conditions. Many years later, Kohout *et al.* [47] reported a similar two-dimensional experiment using 20 mm thick elastic sheets to represent the sea ice, in a 26 m long wave tank with an active control beach to eliminate reflected waves. Passable agreement was found between the data collected and a solution based upon eigenfunction matching at the boundaries of the plates where free-edge conditions were imposed. The experiment is important because the material used to replicate sea ice at the water surface was compliant and flexed rhythmically as the wave train passed down the tank.

A series of three-dimensional wave tank experiments were recently conducted at the École Centrale de Nantes in France to validate the linear scattering theory used to model hydroelastic interactions between regular water waves and sea-ice floes (F. Montiel 2010, personal communication). The simplest experiment involved a single compliant disc, made of expanded polyvinyl chloride, set in motion by a controlled incident wave train generated by a wave maker, but multiple disc experiments were also done. An optical motion tracking device captured the deflection of the disc. This consisted of 39 polystyrene spherical markers placed over half the disc (invoking symmetry), covered with a retro-reflective tape. The motion of these markers was recorded by three infrared cameras. Resistive wave gauges recorded the scattered waves in the water around the disc, which was only allowed to move in heave, roll and pitch, in addition to its flexural response. To the author's knowledge, these are the most sophisticated experiments done to date on the bending of compliant three-dimensional discs in surface gravity waves, serving as a model of a very large floating pontoon or a solitary sea-ice floe. Figure 6 shows snapshots of the bending disc at two different times, below their theoretical counterparts computed using an eigenfunction matching method. Agreement between theory and experiment is impressive.

To complete this section, I mention a unique experiment carried out in the Arctic Environmental Test Basin at the Hamburg Ship Model Basin, Germany [48]. The project reproduced similar but smaller scale work done by Newyear & Martin [49,50]. Being focused on the dispersion and attenuation of

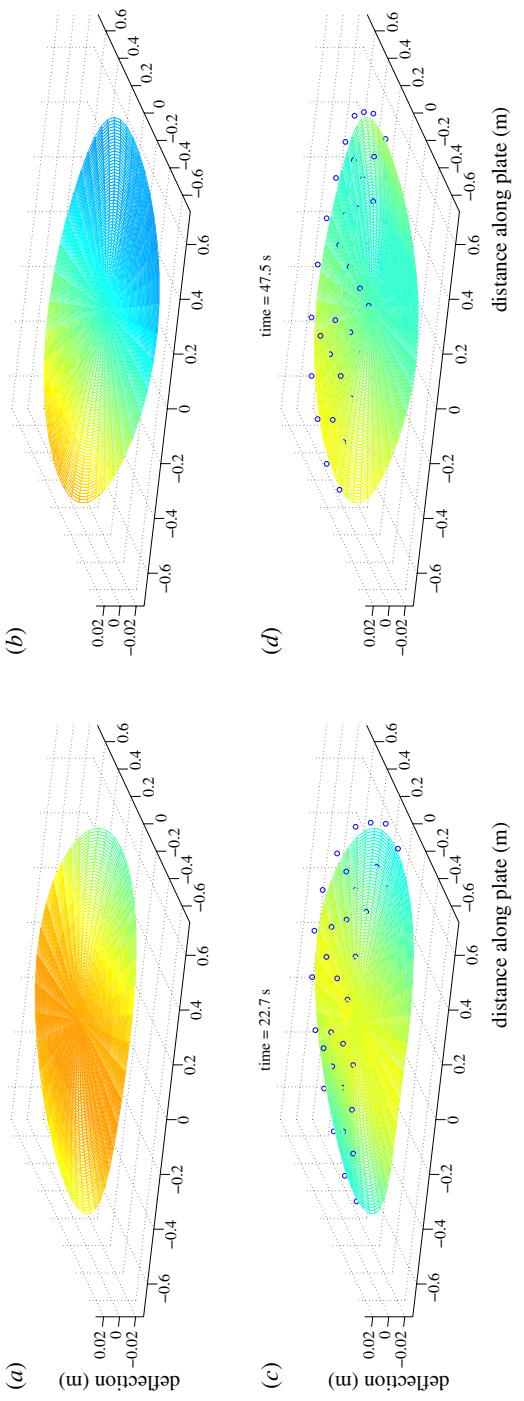

Figure 6. A compliant floating disc deforming under the action of surface gravity waves, at two different times 22.7 s and 47.5 s. Figures (a,b) are computed theoretically, while figures (c,d) come from a set of experiments carried out in the Nantes wave tank. (With thanks to Mr Fabien Montiel.)

surface waves propagating through a grease–pancake ice mixture, it does not strictly relate to hydroelasticity but it has bearing on our earlier discussion about the use of SAR.

There is a paucity of experimental data describing ocean-wave propagation in ice fields, which is particularly troubling as climate warming gradually transforms the Earth's ice-covered oceans to make them more like MIZs.

7. Oceanic general circulation models with sea ice and waves

To assimilate ocean-wave interactions into ice–ocean models or, indeed, within OGCMs, the key challenge is to devise a computationally manageable means of calculating how the many ice floes involved in an archetypal three-dimensional MIZ interact. Some studies attempt to address this problem but each has deficiencies that undermine its efficacy. For example, Boltzmann-type equations in which interactions are in terms of energy alone have been popular, but the underlying energy interaction assumption is naive without coherence effects [51] and, in any case, the resulting equations are still intractable unless unphysical simplifications such as two dimensionality or homogeneity are made. Exact methods that use Graf's formulas and are based upon interaction theory [33] are a candidate but, owing to computational cost, direct application at MIZ scales is implausible. As noted hereinabove, models have consequently previously either been two- [28] or three-dimensional with unrealistic periodicity and averaging [36].

A way forward is to recognize that owing to computational limitations and satellite resolution, ice–ocean models are pixellated into grid cells within which sea-ice descriptors are known only in an average sense across the cell. While obvious, I believe this has not been appreciated before in the context of embedding wave scattering into an ice–ocean model or an OGCM. Accordingly, heterogeneity at subgrid scales, i.e. conglomerations of dissimilar scatterers, is superfluous as only average thickness, floe size and concentration are known. This does not mean that wave scattering does not occur at subgrid scales, or indeed that it does not need to be modelled, but rather that one can gain the immense numerical advantage of assuming that within the cell the morphological parameters that describe the sea ice, namely thickness, floe size and concentration, are uniform. By synthesizing subgrid wave scattering, each cell can then be viewed as a single 'body' with known scattering cross section in the manner of the multi-pole method, and the process repeated by systematically grouping neighbouring cells and determining their interactions until the overall domain has been spanned. Graf's interaction theory can be used for cylindrical geometries but, more generally, boundary-integral equations can provide an instrument to find the interaction of a set of arbitrarily shaped floes or any other scattering sources, which may be used to express a Dirichlet–Neumann map on any contour enclosing the group. The pixellated MIZ visualization will allow all identified key properties—including additional features such as energy dissipation and drift, to be accommodated in a computationally efficient mathematical model, with randomness simulated at each level of the configuration. All aspects of the wave field can be obtained, e.g. the attenuation and evolution of directional spectra.

8. Conclusions

As well as results from embedding wave–ice interaction effects in ice–ocean models and OGCMs, which it is anticipated will improve accuracy and forecasting precision substantially, the next development to occur in the context of hydroelasticity applied to the ice-infested seas relates to large amplitude, i.e. nonlinear, waves. A very small amount of work has been done on this, e.g. Hegarty & Squire [52], which has demonstrated major difficulties as some established methods cannot be extended to higher orders, but the topic is in its infancy. While laboratory experiments relating to single and multiple floating compliant discs have recently begun (§6), there is a dearth of experimental data in the hydroelastic research corpus that needs to be rectified as ocean waves become more fierce and MIZs become more prevalent on a warmer Earth.

V.A.S. acknowledges with gratitude the support of the International Centre for Mathematical Sciences, the University of Otago and the Marsden Fund Council from Government funding administered by the Royal Society of New Zealand.

References

1 Squire, V. A., Dugan, J. P., Wadhams, P., Rottier, P. J. & Liu, A. K. 1995 Of ocean waves and sea ice. *Annu. Rev. Fluid Mech.* **27**, 115–168. (doi:10.1146/annurev.fl.27.010195.000555)
2 Squire, V. A., Vaughan, G. L. & Bennetts, L. G. 2009 Ocean surface wave evolvement in the Arctic Basin. *Geophys. Res. Lett.* **36**, 1–5. (doi:10.1029/2009GL040676)
3 Wadhams, P., Lange, M. A. & Ackley, S. F. 1987 The ice thickness distribution across the Atlantic sector of the Antarctic Ocean in midwinter. *J. Geophys. Res.* **92**, 14 535–14 552. (doi:10.1029/JC092iC13p14535)
4 Serreze, M. C., Holland, M. M. & Stroeve, J. 2007 Perspectives on the Arctic's shrinking sea-ice cover. *Science* **315**, 1533–1536. (doi:10.1126/science.1139426)
5 Kwok, R. & Rothrock, D. A. 2009 Decline in Arctic sea ice thickness from submarine and ICES at records: 1958–2008. *Geophys. Res. Lett.* **36**, L15501 (doi:10.1029/2009GL039035).
6 Wadhams, P., Gill, A. E. & Linden, P. F. 1979 Transects by submarine of the East Greenland Polar Front. *Deep-Sea Res.* **26A**, 1311–1327.
7 NASA. 2010 Earth observatory. See http://earthobservatory.nasa.gov/Features/WorldOfChange/sea_ice_south.php.
8 Vaughan, G. L., Bennetts, L. G. & Squire, V. A. 2009 The decay of flexural-gravity waves in long sea ice transects. *Proc. R. Soc. A* **465**, 2785–2812. (doi:10.1098/rspa.2009.0187)
9 Fung, Y. C. 1965 *Foundations of solid mechanics*. Englewood Cliffs, NJ: Prentice-Hall.
10 Robinson, N. J. & Palmer, S. C. 1990 A modal analysis of a rectangular plate floating on an incompressible liquid. *J. Sound Vib.* **142**, 453–460. (doi:10.1016/0022-460X(90)90661-I)
11 Williams, T. D. & Squire, V. A. 2004 Oblique scattering of plane flexural-gravity waves by heterogeneities in sea-ice. *Proc. R. Soc. Lond. A* **460**, 3469–3497. (doi:10.1098/rspa.2004.1363)
12 Squire, V. A. 2007 Of ocean waves and sea-ice revisited. *Cold Reg. Sci. Technol.* **49**, 110–133. (doi:10.1016/j.coldregions.2007.04.007)
13 Squire, V. A. 2008 Synergies between VLFS hydroelasticity and sea-ice research. *Int. J. Offshore Polar* **18**, 241–253.
14 Williams, T. D. & Squire, V. A. 2006 Scattering of flexural-gravity waves at the boundaries between three floating sheets with applications. *J. Fluid Mech.* **569**, 113–140. (doi:10.1017/S0022112006002552)
15 Williams, T. D. & Squire, V. A. 2008 The effect of submergence on wave scattering across a transition between two floating flexible plates. *Wave Motion* **45**, 361–379. (doi:10.1016/j.wavemoti.2007.07.003)

16 Bennetts, L. G., Biggs, N. R. T. & Porter, D. 2007 A multi-mode approximation to wave scattering by ice sheets of varying thickness. *J. Fluid Mech.* **579**, 413–443. (doi:10.1017/S002211200700537X)
17 Williams, T. D. & Porter, R. 2009 The effect of submergence on the scattering by the interface between two semi-infinite sheets. *J. Fluid Struct.* **25**, 777–793. (doi:10.1016/j.jfluidstructs.2009.02.001)
18 Meylan, M. H. & Squire, V. A. 1996 Response of a circular ice floe to ocean waves. *J. Geophys. Res.* **101**, 8869–8884. (doi:10.1029/95JC03706)
19 Andrianov, A. I. & Hermans, A. J. 2004 Hydroelasticity of elastic circular plate. In *Proc. 19th Int. Workshop on Water Waves and Floating Bodies* (eds M. Landrini, E. F. Campana & A. Iafrati), p. 4. Cortona, Italy: Istituto Nazionale Studi ed Esperienze di Architettura Navale. See http://www.iwwwfb.org/Workshops/19.htm.
20 Meylan, M. H. 2002 Wave response of an ice floe of arbitrary geometry. *J. Geophys. Res.* **107**, 3005. (doi: 10.1029/2000JC000713)
21 Bennetts, L. G., Williams, T. D. & Squire, V. A. 2009 An approximation to wave scattering by an ice polynya. In *Proc. 24th Int. Workshop on Water Waves and Floating Bodies* (ed. A. A. Korobkin), p. 4. Zelenogorsk, Russia: University of East Anglia. See http://www.iwwwfb.org/Workshops/24.htm.
22 Bennetts, L. G. & Williams, T. D. 2010 Wave scattering by ice floes and polynyas of arbitrary shape. *J. Fluid Mech.* **662**, 5–35. (doi:10.1017/S0022112010004039)
23 Wadhams, P. 1986 The seasonal ice zone. In *The geophysics of sea ice* (ed. N. Untersteiner), pp. 825–991. New York, NY: Plenum.
24 Squire, V. A. & Moore, S. C. 1980 Direct measurement of the attenuation of ocean waves by pack ice. *Nature* **283**, 365–368. (doi:10.1038/283365a0)
25 Wang, R. & Shen, H. H. 2010 Gravity waves propagating into an ice-covered ocean: a viscoelastic model. *J. Geophys. Res.* **115**, C06024. (doi:10.1029/2009JC005591).
26 Wadhams, P., Squire, V. A., Ewing, J. A. & Pascal, R. W. 1986 The effect of the marginal ice zone on the directional wave spectrum of the ocean. *J. Phys. Oceanogr.* **16**, 358–376. (doi:10.1175/1520-0485(1986)016<0358:TEOTMI>2.0.CO;2)
27 Wadhams, P., Squire, V. A., Goodman, D. J., Cowan, A. M. & Moore, S. C. 1988 The attenuation of ocean waves in the marginal ice zone. *J. Geophys. Res.* **93**, 6799–6818. (doi:10.1029/JC093iC06p06799)
28 Kohout, A. L. & Meylan, M. H. 2008 An elastic plate model for wave attenuation and ice floe breaking in the marginal ice zone. *J. Geophys. Res.* **113**, C09016. (doi:10.1029/2007JC004434).
29 Peter, M. A. & Meylan, M. H. 2004 Infinite-depth interaction theory for arbitrary floating bodies applied to wave forcing of ice floes. *J. Fluid Mech.* **500**, 145–167. (doi:10.1017/S0022112003007092)
30 Peter, M. A. & Meylan, M. H. 2007 Water-wave scattering by a semi-infinite periodic array of arbitrary bodies. *J. Fluid Mech.* **575**, 473–494. (doi:10.1017/S0022112006004319)
31 Peter, M. A. & Meylan, M. H. 2009 Water-wave scattering by vast fields of bodies. *SIAM J. Appl. Math.* **70**, 1567–1586. (doi:10.1137/090750305)
32 Peter, M. A., Meylan, M. H. & Linton, C. M. 2006 Water-wave scattering by a periodic array of arbitrary bodies. *J. Fluid Mech.* **548**, 237–256. (doi:10.1017/S0022112005006981)
33 Kagemoto, H. & Yue, D. K. P. 1986 Interactions among multiple three-dimensional bodies in water waves: an exact algebraic method. *J. Fluid Mech.* **166**, 189–209. (doi:10.1017/S0022112086000101)
34 Bennetts, L. G. & Squire, V. A. 2009 Wave scattering by multiple rows of circular ice floes. *J. Fluid Mech.* **639**, 213–238. (doi:10.1017/S0022112009991017)
35 Bennetts, L. G. & Squire, V. A. 2010 Linear wave forcing of an array of axisymmetric ice floes. *IMA J. Appl. Math.* **75**, 108–138. (doi:10.1093/imamat/hxp038)
36 Bennetts, L. G., Peter, M. A., Squire, V. A. & Meylan, M. H., 2010 A three-dimensional model of wave attenuation in the marginal ice zone. *J. Geophys. Res.* **115**, C12043. (doi:10.1029/2009JC005982)
37 Masson, D. & LeBlond, P. H. 1989 Spectral evolution of wind-generated surface gravity waves in a dispersed ice field. *J. Fluid Mech.* **202**, 43–81. (doi:10.1017/S0022112089001096)

38 Meylan, M. H., Squire, V. A. & Fox, C. 1997 Towards realism in modelling ocean wave behaviour in marginal ice zones. *J. Geophys. Res.* **102**, 22 981–22 991. (doi:10.1029/97JC01453)

39 Meylan, M. H. & Masson, D. 2006 A linear Boltzmann equation to model wave scattering in the marginal ice zone. *Ocean Model.* **11**, 417–427. (doi:10.1016/j.ocemod.2004.12.008)

40 Doble, M. J., Mercer, D. J. L., Meldrum, D. T. & Peppe, O. C. 2006 Wave measurements on sea ice: developments in instrumentation. *Ann. Glaciol.* **44**, 108–112. (doi:10.3189/172756406781811303)

41 Wadhams, P. & Doble, M. J. 2009 Sea ice thickness measurement using episodic infragravity waves from distant storms. *Cold Reg. Sci. Technol.* **56**, 98–101. (doi:10.1016/j.coldregions.2008.12.002)

42 Liu, A. K., Vachon, P. W., Peng, C. Y. & Bhogal, A. S. 1992 Wave attenuation in the marginal ice zone during LIMEX. *Atmos. Ocean.* **30**, 192–206. (doi:10.1080/07055900.1992.9649437)

43 Wadhams, P., Parmiggiani, F. E. & de Carolis, G. 2002 The use of SAR to measure ocean wave dispersion in frazil-pancake icefields. *J. Phys. Oceanogr.* **32**, 1721–1746. (doi:10.1175/1520-0485(2002)032<1721:TUOSTM>2.0.CO;2)

44 Wadhams, P., Parmiggiani, F. E., de Carolis, G., Desiderio, D. & Doble, M. J. 2004 SAR imaging of wave dispersion in Antarctic pancake ice and its use in measuring ice thickness. *Geophys. Res. Lett.* **31**, L15305. (doi:10.1029/2004GL020340)

45 Squire, V. A. 2003 Numerical modelling of realistic ice floes in ocean waves. *Ann. Glaciol.* **4**, 277–282.

46 Wadhams, P. 1973 The effect of a sea ice cover on ocean surface waves. PhD thesis, University of Cambridge, Cambridge, UK.

47 Kohout, A. L., Meylan, M. H., Sakai, S., Hanai, K., Leman, P. & Brossard, D. 2007 Linear water wave propagation through multiple floating elastic plates of variable properties. *J. Fluid Struct.* **23**, 649–663. (doi:10.1016/j.jfluidstructs.2006.10.012)

48 Wang, R. & Shen, H. H. 2010 Experimental study on surface wave propagating through a grease-pancake ice mixture. *Cold Reg. Sci. Technol.* **61**, 90–96. (doi:10.1016/j.coldregions.2010.01.011)

49 Newyear, K. & Martin, S. 1997 A comparison of theory and laboratory measurements of wave propagation and attenuation in grease ice. *J. Geophys. Res.* **102**, 25 091–25 100. (doi:10.1029/97JC02091)

50 Newyear, K. & Martin, S. 1999 Comparison of laboratory data with a viscous two-layer model of wave propagation in grease ice. *J. Geophys. Res.* **104**, 7837–7840. (doi:10.1029/1999JC900002)

51 Berry, M. V. & Klein, S. 1997 Transparent mirrors: rays, waves and localization. *Eur. J. Phys.* **18**, 222–228. (doi:10.1088/0143-0807/18/3/017)

52 Hegarty, G. M. & Squire, V. A. 2008 A boundary integral method for the interaction of large amplitude waves with a compliant floating raft such as a sea-ice floe. *J. Eng. Math.* **62**, 355–372. (doi:10.1007/s10665-008-9219-1)